Microstructure and residual strain in runned railway wheel investigated by neutron diffraction

Wu Shengchuan[1)] Xu Pingguang[2)]

[1)]Southwest Jiaotong University [2)]Japan Atomic Energy Agency

The axial, hoop, and radial gradient residual stress inside the axles were measured by neutron diffraction. Experiment results show that approximately -515 MPa (axial), -710 MPa (hoop), and -43 MPa (radial) residual stress was retained underneath the surface. When the axle samples contain fatigue cracks, relaxation of the compressive residual stresses in the surface layer occurs.

key words: Compressive residual stress; Neutron diffraction; Fatigue crack propagation

1. Objectives

Induction-hardened carbon steel S38C railway axles are mainly used in the Japanese Shinkansen and early CRH2-type high-speed EMU of China. These axles were processed with the high-frequency induction quenching technology, which introduces a large layer depth of compressive residual stresses, along with the phase transformation of the surface material from ferrite to martensite. Gradient residual stress with several millimeters is retained in middle carbon S38C axles after induction hardening, which has become a critical concern for fatigue structural integrity. Because the neutron beam has an extremely strong penetration capacity and has prominent advantages in the characterization of deep residual stresses in large components. Experiments such as neutron diffraction were carried out, along with *quasi-in-situ* neutron diffraction experiments to characterize the residual stress changes in three-point bending fatigue samples of S38C axles containing fatigue cracks of different depths.

2. Methods

As shown in Fig. 1, the neutron diffraction experiment was performed at a dedicated neutron diffractometer for Residual Stress Analysis of Engineering Materials (RESA), at the Japan Atomic Energy Agency (JAEA). To calculate the residual stress distribution, the measured specimen was repositioned three times for the three vector directions. Measurement conditions are taken for the three-diffraction vector in axial, hoop and radial directions, diffraction plane is 211, nominal wavelength is 1.6852 ± 0.0002 Å, and gauge volume is 2×2×2 mm^3. Considering test results could reflect the stress gradient well, and to avoid empty volumes, it was decided all three directions were in the middle of the axial cross-section of the specimens, with the test points at 1, 1.5, 2, 3, 5, and 7 mm depths from the axle surface.

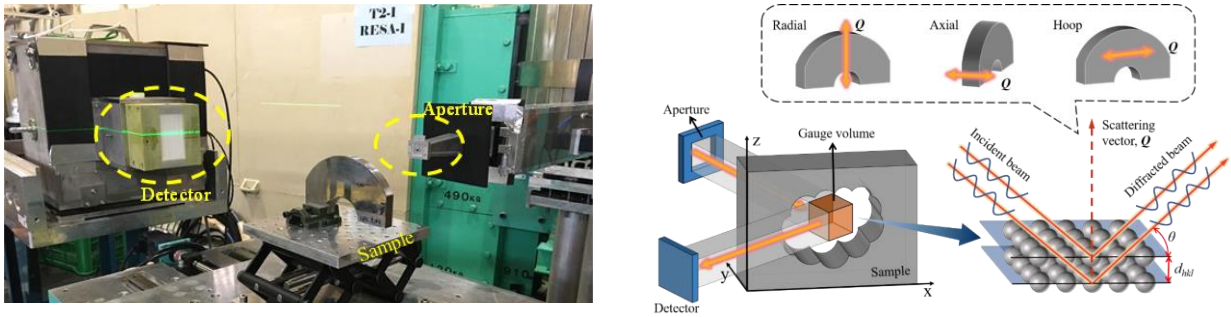

a) Experimental photograph of neutron diffraction measurements.

b) Schematic illustration for the triaxial orientation set up of S38C axle samples in RESA angle dispersive neutron diffraction experiment

Fig. 1 S38C Axle Neutron Diffraction Tests and Schematic Diagrams

3. Results and Discussion

According to the results of neutron diffraction experiments, high levels of tangential and axial initial compressive residual stresses exist in the surface layer of S38C axles due to martensitic phase transformation in the surface layer of the axles during the induction hardening process. For example, a compressive residual stress of 515 MPa in the axial direction and 710 MPa in the tangential direction was observed at a depth of 1 mm from the surface layer, followed by a gradual transition to tensile residual stress. When the axle samples contained fatigue cracks, relaxation of the compressive residual stresses in the surface layer occurred. As the crack length increases, the relaxation becomes more and more significant, and the compressive residual stresses introduced by induction hardening in the axle are completely released and gradually stabilized when the crack depth increases to 6 mm.

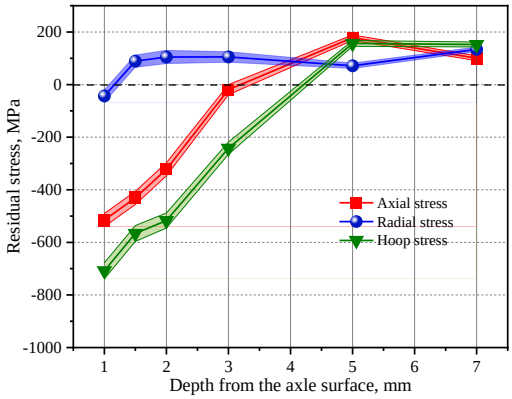

a) In-depth residual stress distribution inside a real railway S38C hollow axle.

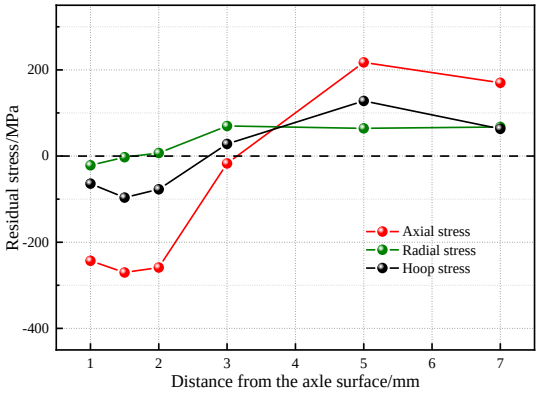

b) Residual stress distribution with 1 mm depth fatigue cracks.

Fig. 2 Evolution of residual stress after fatigue crack initiation on axle.

4. References

[1] James MN, Hughes DJ, Chen Z, Lombard H, Hattingh DG, Asquith D, Yates JR, Webster PJ. Residual stresses and fatigue performance. Eng Fail Anal, 2007; 14(2): 384-395.

[2] Withers PJ, Turski M, Edwards L, Bouchard PJ, Buttle DJ. Recent advances in residual stress measurement. Int J Pres Ves Pip, 2008; 85(3): 118-127.

[3] Schajer GS, Prime MB, Withers PJ. Why is it so challenging to measure residual stresses? Exp Mech, 2022; 62(9): 1521-1530.

[4] Hojo T, Akiyama E, Saitoh H, Shiro A, Yasuda R, Shobu T, Kinugasa J, Yuse F. Effects of residual stress and plastic strain on hydrogen embrittlement of a stretch-formed TRIP-aided martensitic steel sheet. Corros Sci, 2020; 177: 108957.

[5] Harjo S, Tomota Y, Ono M. Measurements of thermal residual elastic strains in ferrite–austenite Fe–Cr–Ni alloys by neutron and X-ray diffractions. Acta Mater, 1998; 47(1): 353-362.

[6] Ojima M, Inoue J, Nambu S, Xu PG, Akita K, Suzuki H, Koseki T. Stress partitioning behavior of multilayered steels during tensile deformation measured by in situ neutron diffraction. Scr Mater, 2012; 66(3-4), 139-142.

[7] Xu PG, Harjo S, Ojima M, Suzuki H, Ito T, Gong W, Akita K. High stereographic resolution texture and residual stress evaluation using time-of-flight neutron diffraction. J Appl Crystallogr, 2018; 51(3), 746-760.

[8] Qin TY, Hu FF, Xu PG, Zhang H, Zhou L, Ao N, Su YH, Shobu T, Wu SC. Gradient residual stress and fatigue life prediction of induction hardened carbon steel axles: Experiment and simulation. International Journal of Fatigue, 2024: 108336.